Journal of Statistical Physics, Vol. 71, Nos. 1/2, 1993

Directed Polymer Melts and Quantum Critical Phenomena

Randall D. Kamien[1,2] and David R. Nelson[1]

Received June 19, 1992; final October 22, 1992

The statistical mechanics of directed linelike objects, such as directed polymers in an external field, strands of dipoles in both ferro- and electrorheological fluids, and flux lines in high-T_C superconductors, bears a close resemblance to the quantum mechanics of bosons in $2+1$ dimensions. We show that single-component and binary mixture critical phenomena in these systems are in the universality class of three-dimensional uniaxial dipolar ferromagnets and ferroelectrics. Our results also apply to films of two superfluid species undergoing phase separation well below their λ-points near $T=0$. In the case of directed polymers and electrorheological fluids we analyze the effects of free ends occurring in the sample as well as a novel directionally-dependent compressibility.

KEY WORDS: Quantum critical phenomena; directed polymers; critical mixing; phase transitions.

1. INTRODUCTION AND SUMMARY

There has recently been renewed interest in the analogy between the classical statistical mechanics of lines and the quantum mechanics of bosons in $2+1$ dimensions.[1] Configurations of directed lines can be mapped onto the world lines of a collection of bosons in one fewer dimension. Examples include flux lines in high-temperature superconductors,[2] polymer nematics in a strong external field, and ferro- and electrorheological fluids.[3,4]

These systems can be modeled by a free energy of the form (see ref. 5 for a review)

$$F=\int dz\, d^2r \left[\frac{h}{2}\mathbf{t}^2+\frac{e}{2}(\nabla_\perp \delta\rho)^2+\frac{\alpha}{2}(\partial_z \delta\rho)^2+\frac{b}{2}\delta\rho^2+\frac{w}{3!}\delta\rho^3+\frac{c}{4!}\delta\rho^4\right] \quad (1.1)$$

[1] Lyman Laboratory of Physics, Harvard University, Cambridge, Massachusetts 02138.
[2] Present address: School of Natural Sciences, Institute for Advanced Study, Princeton, New Jersey 08540.

0022-4715/93/0400-0023$07.00/0

The partition function

$$Z = \int [d\mathbf{t}][d\delta\rho]\, e^{-F/k_B T} \tag{1.2}$$

is subject to the constraint

$$\partial_z \delta\rho + \nabla_\perp \cdot \mathbf{t} = 0 \tag{1.3}$$

where $\delta\rho(\mathbf{r}, z) = \rho(\mathbf{r}, z) - \rho_0$ is a cross-sectional areal density deviation from its average value ρ_0 in a plane perpendicular to z, and $\mathbf{t}(\mathbf{r}, z)$ is a tangent field in the same plane. Given a microscopic description of directed polymers, via their trajectories defined by single-valued functions $\{\mathbf{r}_j(z)\}$ along the z-axis, $\rho(\mathbf{r}, z)$ and $\mathbf{t}(\mathbf{r}, z)$ are defined by (see Fig. 1)

$$\rho(\mathbf{r}, z) = \sum_i \delta^2[\mathbf{r} - \mathbf{r}_i(z)] \tag{1.4}$$

and

$$\mathbf{t}(\mathbf{r}, z) = \sum_i \frac{d\mathbf{r}_i(z)}{dz} \delta^2[\mathbf{r} - \mathbf{r}_i(z)] \tag{1.5}$$

We assume that, as external parameters such as field strength, osmotic pressure, temperature, solvent quality, etc., are varied, the polynomial part of (1.1) in $\delta\rho$ exhibits a line of first-order phase transitions from a high- to low-density phase, terminating in a second-order phase transition. Along the critical isochore $w = 0$, and b then changes sign at the mean field critical point. Here and throughout, we distinguish the z direction as the direction along which the lines are aligned, and denote by $\nabla_\perp$ the derivative

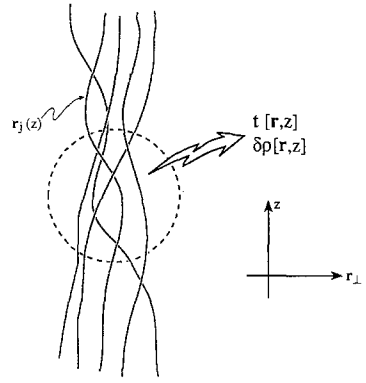

Fig. 1. Hydrodynamic volume averaging over directed lines in $d+1$ dimensions which leads to the coarse-grained density and tangent fields used in this paper.

perpendicular to the z axis. Additionally, we use boldface to denote vectors in the perpendicular plane. In the case of quantum mechanical bosons, we think of the z direction as a timelike axis along which particle world lines are extended. Planck's constant $\hbar$ plays the role of "temperature" in this system, $\beta\hbar$ is the sample thickness, and the coupling h is the inverse "mass density" of the bosons.

The constraint (1.3) in the context of polymers corresponds to the absence of polymer free ends,[3,4] that is, conservation of polymer number as we move up the z axis. In the context of quantum mechanical bosons, this constraint merely sets $\mathbf{t}$ to be the canonical momentum density of the particles.[4] Models similar to (1.1) were first posed as Landau–Ginzburg-type theories,[2,6–8] but were later shown to be a direct consequence of the boson mapping.[4]

In fact, this model is equivalent to a three-dimensional uniaxial dipolar ferroelectric (or ferromagnet) near its critical point, first studied in 1969 by Larkin and Khmel'nitskiĭ.[9] To see this, we use the constraint (1.3) to solve for the longitudinal part of $\mathbf{t}$. Upon integrating out the transverse part of $\mathbf{t}$ we obtain an effective free energy

$$F_{\text{eff}} = \frac{1}{2}\int \frac{dq_z}{2\pi}\frac{d^2q_\perp}{(2\pi)^2}\left(h\frac{q_z^2}{q_\perp^2} + eq_\perp^2 + \alpha q_z^2 + b\right)|\delta\rho(q_\perp, q_z)|^2 + \frac{c}{4!}\int dz\, d^2r(\delta\rho)^4 \tag{1.6}$$

where the quadratic part has been written in Fourier space. Here and henceforth, we restrict our attention to the critical isochore, and set $w = 0$. Equation (1.6) is the familiar form of the Landau theory for a uniaxial Ising ferromagnet or ferroelectric with a mean field critical point at $b = 0$.[9]

A model very similar to (1.1) applies to polymer nematics in which the external field is turned off, so that the alignment represents a *spontaneously* broken symmetry instead of being externally imposed.[3,4,6,8] In this case, $\mathbf{t}(\mathbf{r}, z)$ represents a nematic director field and the term $\frac{1}{2}h\mathbf{t}^2$ is replaced by the usual nematic gradient free energy.[10] Simple power counting arguments for this model suggest that nonclassical critical behavior results below $(3+1)$ dimensions. A complete treatment, however, would require a discussion of the effects of hairpin turns in the polymer configurations.[4] We restrict our attention here to polymer nematics in a strong external field, and to length scales less than the spacing between hairpins, to avoid these complications.

1.1. Electrorheological Fluids and the Effect of Free Ends

The effective attraction for polymers in a nematic solvent is similar to the fluctuation-induced attraction of strings of colloidal spheres discussed

by Halsey and Toor.[11] This attractive part of the interchain potential in electrorheological fluids can be offset by a hard-core repulsion at short distances, and may be adjusted by varying the dielectric constant of the solvent. Since an electric field is required to create directed strings of dielectric spheres, hairpin configurations will be greatly suppressed in electrorheological fluids, as there is no longer an up–down symmetry. We then expect that (1.1) is especially apt for these systems, once free ends are taken into account. Halsey and Toor,[12] by considering the bulk energetics of the system, have argued that at sufficiently large fields, the electrorheological strings will phase separate, leading to two-phase coexistence. The critical point discussed here would then describe a transition to a uniform density of coexisting liquid and gas dielectric strings.

To study this point further, consider the free energy at fixed potential due to the electric field

$$U = -\frac{1}{8\pi}\int dz\, d^2\mathbf{r}\, \varepsilon[n(\vec{x})]\, \vec{E}^2(\vec{x}) \tag{1.7}$$

where n is the full three-dimensional colloid density, and $\varepsilon(n)$ is the effective dielectric constant. There is an overall minus sign because this is the energy at fixed $\vec{E}$. Since $d^2\varepsilon(n)/dn^2 > 0$,[3] it is energetically favorable to phase separate into dense and dilute regions. However, at finite temperature, configurational entropy plays a role. Certainly, at fixed electric field, the temperature can be increased until entropy dominates and there is only one uniform phase of directed lines. However, entropy also favors shorter chains at such temperatures, which could obscure the entanglement effects which are the main focus of this paper (see below).

Recent numerical simulations by Tao[14] suggest that at fixed temperature there are actually two critical electric fields, E_{C1} and E_{C2} ($E_{C2} < E_{C1}$). Below E_{C2} the fluid consists primarily of a gas of monomers. Above E_{C1} the colloidal particles clump together and phase separate into "columns" and dilute chains as Halsey and Toor's argument would suggest. The columns may in fact be crystalline.[14,15] Between E_{C2} and E_{C1} there are dense strings of colloidal spheres with random positions in any constant-z cross section. The simulation suggests a first-order phase

[3] For a system of spheres arranged in a cubical lattice or amorphously, the Clausius–Mosotti relation holds, so $\varepsilon(n) = (1 + 2v\gamma n)/(1 - v\gamma n)$, where γ is the molecular polarizability and v is the molecular volume. In this case $(d^2\varepsilon/dn^2)(n)$ is explicitly positive. A virial expansion for the bulk dielectric constant in terms of the density can be done in general. The first virial term leads to the Clausius–Mosotti relation, and the second term is generally quite small. Thus $(d^2\varepsilon/dn^2)(n)$ is expected to be positive even if the spheres are not arranged either cubically or randomly. See ref. 13.

transition from the random line phase to the clumped phase. At lower densities, experimental measurements do not suggest crystalline order in the columns.[16] Thus, at low enough densities we can have coexistence of liquidlike columns and a gas of chains, possibly terminating in a critical point.

One shortcoming of our model in its present form is that the chains it describes must start and stop at the boundaries of the sample. Both directed polymers and colloidal chains should be allowed to have free ends within the sample. As discussed in Section 4, free ends may be incorporated by relaxing the constraint (1.3) and using the free energy[3–5]

$$F = \int dz\, d^2x \left[\frac{h}{2}\mathbf{t}^2 + \frac{e}{2}(\nabla_\perp \delta\rho)^2 + \frac{\alpha}{2}(\partial_z \delta\rho)^2 \right.$$
$$\left. + \frac{b}{2}\delta\rho^2 + \frac{c}{4!}\delta\rho^4 + \frac{G}{2}(\partial_z \delta\rho + \nabla_\perp \cdot \mathbf{t})^2 \right] \tag{1.8}$$

By taking $G \to \infty$, we recover our original model. Additionally, it can be shown that $G \sim l$ as $l \to \infty$, where l is the average chain length.[3,4] The crossover from elongated objects to point objects when the chains are finite will be discussed in detail in Section 4.

1.2. Phase Separation in the Flux Liquid Phase

Flux lines in superconductors may also be described by an analogy with bosons.[2] However, in the absence of magnetic monopoles, flux lines cannot have free ends inside the sample. Their behavior, then, is much closer to the behavior of quantum mechanical bosons, as the constraint (1.3) is always satisfied.

Calculations to date for fluctuating flux lines have assumed a purely repulsive pair potential.[2] Muzikar and Pethicke,[17] however, have argued that an effective attractive interaction arises under some circumstances near H_{C1} in the extreme type II limit. This interaction would convert the continuous onset of flux penetration at H_{C1} to a first-order transition. An even more intriguing situation would arise if the interaction between the flux lines had *two* distinct minima (see the inset to Fig. 3). In this case, there should be a first-order transition at H_{C1}, and a line separating *two* coexisting flux liquid phases, as in Fig. 2. Our theory applies to the critical point marking the terminus of this first-order phase boundary. The critical isochore is shown as a dotted line in the figure.

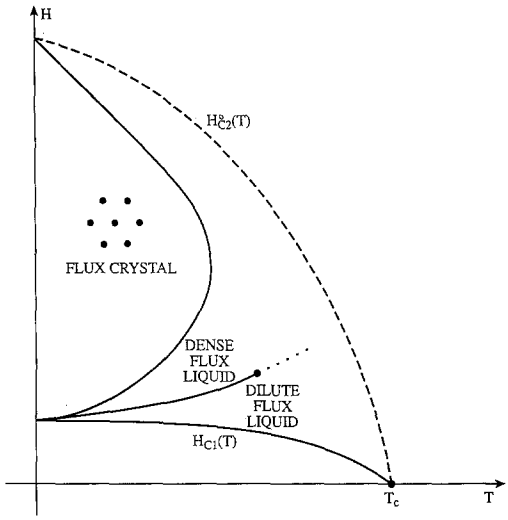

Fig. 2. Speculative phase diagram for type II superconductors with an attractive double well interaction between flux lines (see the inset to Fig. 3) which allows for coexisting dense and dilute entangled flux liquids. At sufficiently high temperatures, this line terminates in a critical point. The critical isochore, which marks the extension of this line into the single-phase region, is shown as a dotted line.

1.3. Quantum Critical Phenomena

Our analysis, of course, can also be applied directly to boson systems at $T=0$, which are equivalent to infinitely long directed polymers.[1] In the case of a single particle species, we would be describing the terminus of a line of first-order transitions separating superfluids coexisting at two different densities. How this situation might come about is illustrated in Fig. 3. The inset shows an unusual pair potential with *two* distinct minima describing particles which, like helium, are light enough to avoid crystallization at $T=0$ at low pressures. The two minima lead to two distinct liquid phases with increasing pressure. At low pressures, the stable zero-temperature liquid has near neighbors occupying the deeper, outermost minimum. As pressure is increased, there is a first-order phase transition to a denser liquid with the innermost minimum occupied, followed eventually by crystallization at even higher pressure. The two liquids must be superfluids at $T=0$. In Fig. 3, the parameters have been adjusted so that the critical point for the dilute and dense superfluids $S1$ and $S2$ occurs below the dashed λ-line describing the transition to a normal liquid with increasing temperature. There is a second critical point associated with the coexistence of this normal liquid with a dilute gas.

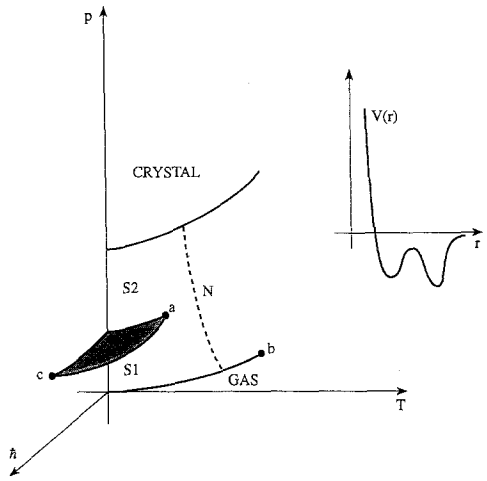

Fig. 3. Pressure–temperature phase diagram for a quantum fluid with the unusual pair potential shown in the inset. The outer minimum dominates in the superfluid phase $S1$, while the inner minimum is primarily occupied in the higher-pressure superfluid $S2$. Phases $S1$ and $S2$ are separated from a normal liquid N by the dashed λ-line. Points a and b are conventional critical points. By enhancing quantum fluctuations at $T=0$ (say, by increasing $\hbar$), one arrives at the critical point c discussed in the paper.

To obtain the critical point of interest to us here, we must increase $\hbar$ (or decrease the mass) at $T=0$ until the two superfluid liquid phases become indistinguishable as at the point c in the figure. Although this *gedanken* experiment is clearly rather esoteric, some control over quantum fluctuations may be achievable for two-dimensional helium films, where out-of-plane fluctuations alter the effective two-body potential. By varying the type of substrate, it may be possible to create a purely repulsive effective potential and a novel superfluid gas phase at $T=0$.[18],[4] We should stress, however, that we do not expect the unusual phase diagram of Fig. 3 for *either* purely repulsive potentials or conventional helium potentials with a single minimum. What happens as the depth of the single minimum in a helium-like potential is decreased to approach the limit of a purely repulsive potential[18] is a separate but also interesting question. The behavior in this case is described by a quantum tricritical point which is discussed in Appendix B.

The density operator of the bosons described above is given by (1.4). Upon differentiating with respect to z we have

[4] See, however, recent work by C. Carrero and M. Cole [*Phys. Rev. B* **46**:10947 (1992)] for evidence *against* this hypothesis.

$$\partial_z \rho(\mathbf{r}, z) = -\sum_i \frac{d\mathbf{r}_i(z)}{dz} \cdot \nabla_{\perp,\mathbf{r}} \delta^2[\mathbf{r} - \mathbf{r}_i(z)]$$

$$= -\nabla_\perp \cdot \sum_i \frac{d\mathbf{r}_i(z)}{dz} \delta^2[\mathbf{r} - \mathbf{r}_i(z)] \tag{1.9}$$

The final sum on the right-hand side is just (1.5), so we have derived (1.3). The quantity

$$\mathbf{t}(\mathbf{r}, z) = \sum_i \frac{d\mathbf{r}_i(z)}{dz} \delta^2[\mathbf{r} - \mathbf{r}_i(z)]$$

is just the momentum operator of the bosons.[2,4] On a more formal level, note that the "time dependence" (i.e., the z dependence) of the quantum operator (1.4) is given by the (Wick rotated) Heisenberg equation of motion,

$$\partial_z \rho(\mathbf{r}, z) = [\rho(\mathbf{r}, z), \mathscr{H}] \tag{1.10}$$

where $\mathscr{H}$ is the underlying quantum Hamiltonian. Upon identifying (1.1) with the integral over imaginary time of the coarse-grained hydrodynamic Lagrangian associated with this Hamiltonian (as is appropriate for finite-temperature quantum statistical mechanics), we recover (1.3) from (1.10) upon using the commutation relation between $\rho(\mathbf{r}, z)$ and $\mathbf{t}(\mathbf{r}, z)$,

$$[\rho(\mathbf{r}, z), \mathbf{t}(\mathbf{r}', z)] = \frac{k_B T}{h} \nabla_\perp \delta^2(\mathbf{r} - \mathbf{r}') \tag{1.11}$$

In the hydrodynamic limit considered here, this commutator becomes the classical "Poisson bracket" relation between density and momentum, which arises because the momentum operator is the generator of translations.[19],[5] The constraint (1.3) thus directly reflects the noncommutivity of the underlying position and momentum operators.

Note also that our results represent a new universality class for Ising-like quantum critical phenomena. A related type of quantum critical phenomenon, extensively studied in the past,[20] arises for the Ising model in a transverse magnetic field. The quantum Hamiltonian defined on a hypercubical lattice in d dimensions is

$$\mathscr{H} = -J \sum_{\langle i,j \rangle} \sigma_i^z \sigma_j^z - h \sum_j \sigma_j^x \tag{1.12}$$

[5] See also the treatment of bosons in ref. 20, pp. 6–8.

where the $\{\vec{\sigma}_i\}$ are Pauli spin matrices. The ordered state at $T=0$ is destroyed for sufficiently large h. This disordering transition is known to be in the universality class of the $(d+1)$-dimensional classical Ising model.[21] Equation (1.12) describes a quantum lattice gas, with the world lines of the "particles" (up spins, say) in a $T=0$ path integral formulation representing the directed polymers discussed in this paper. Because the σ_j^x is a spin flip operator, these "polymers" stop and start at random in $(d+1)$ dimensions. The appropriate coarse-grained Landau description would be similar to (1.1) *without*, however, the constraint (1.3). The spin flip operator in (1.12) does not respect this conservation law, so it is not surprising that we find a different universality class for boson critical phenomena. Introducing free ends in our model has the same effect as the spin flip operator in (1.12). As discussed above, we then find a crossover from the $(d+1)$-dimensional uniaxial dipolar Ising critical phenomena to the $(d+1)$-dimensional Ising behavior expected for (1.12).

1.4. Directed Polymer Blends and Quantum Binary Mixtures

By extending the original model to allow for binary mixtures, we can study the consolute point of two different directed polymer species. In particular, we can determine the critical exponents near the demixing point of directed polymer blends and compare them to those for point particles. Analogous phenomena should occur in binary mixtures of two different superfluids. Among the possible candidates would be films of ^{6}He and He^4 or possibly, a superfluid monolayer of spin aligned hydrogen mixed with superfluid He^4. As the mass ratio m_1/m_2 of the two species is increased toward unity with $\hbar > 0$, quantum fluctuations should eventually cause the two superfluids to mix. The same effect may be achievable by varying the properties of the substrate or formally, by increasing $\hbar$. A phase diagram as a function of temperature, composition, and $\hbar$ is shown in Fig. 4. Note the incomplete phase separation appearing for nonzero $\hbar$. The theory applies to the critical point at $T=0$. In Section 5 we will analyze such binary mixtures in greater detail. Although we shall concentrate on $2+1$ quantum systems, our results are easily adapted to $(3+1)$-dimensional quantum problems which are well described by mean field theory (see Section 4).

1.5. Outline

In Section 2 we formulate the Landau theory that will be the focus of this paper. We follow the derivation developed in ref. 4 for flux lines, which leads to a coherent-state functional integral. From there we describe the hydrodynamic theory with and without free ends as in ref. 4. In

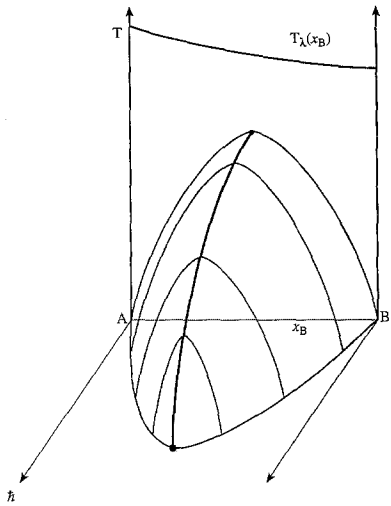

Fig. 4. Phase diagram for a binary mixture of two superfluid species as a function of the concentration of species B, temperature, and Planck's constant. This paper addresses the nature of the critical point which occurs at $T=0$.

Appendix A we present a similar derivation for two interacting polymer species.

In Section 3 we describe the correlation functions of this theory which could be measured by x-ray or neutron diffraction experiments. We also discuss the meaning of the direction-dependent compressibility which characterizes these directed line systems.

In Section 4 we study the critical behavior of our model via an expansion in $2-\varepsilon+1$ dimensions. We reproduce the results of Larkin and Khmel'nitskiĭ for $\varepsilon=0$ when there are no free ends[9] and find that free ends are a relevant perturbation leading to the critical behavior of a $(d+1)$-dimensional Ising model with short-range interactions.

Finally, in Section 5 we discuss the critical mixing of two polymer or quantum boson species. Using the free energy derived in Appendix A, we show that, just as in the point-particle case, the critical mixing of linelike objects is in the same universality class as single-component critical phenomena.

Appendix B discusses how the transition at $T=0$ from a vacuum to a superfluid gas changes to a transition from a vacuum to a superfluid liquid when a purely repulsive pair potential acquires a single minimum of sufficient depth.

2. COHERENT-STATE FUNCTIONAL INTEGRALS AND LANDAU THEORY

The derivation of (1.1) from a more microscopic free energy for directed lines follows the presentations in refs. 2 and 4. We only outline the main points here, first reviewing the theory for chains which span the system. Internal free ends are then introduced by adding a source to the boson coherent-state field theory.[3,4]

We start from the following path integral partition function for the N chains:

$$Z_N = \frac{1}{N!} \int \prod_{i=1}^{N} [d\mathbf{r}_i] \times \exp\left\{ -\frac{1}{k_B T} \int_0^L dz \left[\sum_{i=1}^{N} \frac{g}{2} \left(\frac{d\mathbf{r}_i}{dz} \right)^2 + \sum_{i<j}^{N} V[\mathbf{r}_i(z) - \mathbf{r}_j(z)] \right] \right\} \tag{2.1}$$

where we have restricted our attention to interactions between lines through an equal "time" potential $V[\mathbf{r}_i(z) - \mathbf{r}_j(z)]$.

The boson field theory is derived in three steps. We first write the transfer matrix associated with (2.1) in terms of a many-particle real-time Schrödinger equation for the polymer positions, and then second quantize this equation using bosons. Finally, we pass to a coherent-state functional integral representation of the second quantized formalism.

The grand canonical partition sum which results is

$$Z_{gr} \equiv \sum_{N=0}^{\infty} e^{L\mu N/k_B T} Z_N = \int [d\psi][d\psi^*]\, e^{-S[\psi^*, \psi]} \tag{2.2}$$

where $\psi(\mathbf{r}, z)$ is a complex boson field. The boson action S reads

$$S = \int_0^L dz \int d^2 r \left[\begin{array}{l} \psi^*(\mathbf{r}, z)(\partial_z - D\nabla_\perp^2 - \bar{\mu})\, \psi(\mathbf{r}, z) \\ + \frac{1}{2} \int d^2 r'\, \bar{v}(\mathbf{r} - \mathbf{r}')\, |\psi(\mathbf{r}, z)|^2\, |\psi(\mathbf{r}', z)|^2 \end{array} \right] \tag{2.3}$$

where $D = k_B T/2g$, $\bar{\mu} = \mu/k_B T$, and $\bar{v} = V/k_B T$. Standard manipulations show that the density of flux lines is

$$\rho(\mathbf{r}, z) = |\psi(\mathbf{r}, z)|^2 \tag{2.4}$$

2.1. Entangled Limit with Free Ends

We now assume that all phases are dense enough to be entangled, and expand around the mean density ρ_0. For polymers of length l, entangle-

ment means $(Dl)^{1/2} \gg \rho_0^{-1/2}$, while for quantum systems, we require very low temperatures so that the thermal de Broglie wavelength is large compared to the particle spacing. We parametrize the field ψ by $\psi = \sqrt{\rho}\, e^{i\theta}$, a change of variables with unit functional determinant, and find from (2.3) that

$$S = \int dz\, d^2r \left[\frac{D(\nabla_\perp \rho)^2}{4\rho} + D\rho(\nabla_\perp \theta)^2 + i\rho\partial_z\theta - \bar{\mu}\rho + \frac{v}{2}\rho^2 \right] \tag{2.5}$$

Upon introducing an auxiliary field $\mathbf{t}(\mathbf{r}, z)$ conjugate to $\nabla_\perp\theta(\mathbf{r}, z)$ via a Hubbard–Stratonovich transformation, and integrating out $\theta(\mathbf{r}, z)$, we arrive at the partition sum (1.2).[4,22] See Appendix A for the analogous transformation applied to binary mixtures of quantum bosons.

We can add a (Poisson distribution) of free ends to the theory by adding to the action (2.3) a term of the form[3]

$$\begin{aligned} \delta S &= -\eta \int dz\, d^2r [\psi(\mathbf{r}, z) + \psi^*(\mathbf{r}, z)] \\ &= -\int dz\, d^2r\, 2\eta \sqrt{\rho} \cos\theta \end{aligned} \tag{2.6}$$

The mean polymer length l is related to η by $2\eta l k_B T = \sqrt{\rho_0}$.[4] We may expand this term in powers of θ if the fluctuations in θ are small, which they will be if the polymers are sufficiently dense and entangled. To leading order in θ, Eq. (2.6) becomes

$$\delta S \approx \text{const} + \int dz\, d^2r\, \eta \sqrt{\rho}\, \theta^2 \tag{2.7}$$

The Hubbard–Stratonovich transformation now leads to

$$S = \int dz\, d^2r \left\{ \frac{D\mathbf{t}^2}{\rho} + \frac{D(\nabla_\perp \rho)^2}{4\rho} - \bar{\mu}\rho + \frac{v}{2}\rho^2 + \frac{1}{4\eta\sqrt{\rho}} [\partial_z \rho + \nabla_\perp \cdot \mathbf{t}]^2 \right\} \tag{2.8}$$

Upon expanding around an average density ρ_0, we arrive at the theory for finite-length polymers (1.8), with $G = 1/4\eta\sqrt{\rho_0}$ and $h = 2D/\rho_0$.

3. CORRELATIONS AND COMPRESSIBILITY

From the free energy (1.8) we can, by considering only quadratic terms, easily find the hydrodynamic form of the structure function, which could be measured by either neutron or x-ray diffraction. Here and hence-

forth we change units so that $e=1$. The Fourier-transformed density–density correlation function is then

$$S(q_\perp, q_z) = \frac{\langle \delta\rho(q_\perp, q_z)\, \delta\rho(-q_\perp, -q_z)\rangle}{\rho_0^2}$$
$$= \frac{k_B T(h + Gq_\perp^2)}{(G\alpha q_\perp^2 + Gh + \alpha h)\, q_z^2 + (Gb + h)\, q_\perp^2 + Gq_\perp^4 + hb} \tag{3.1}$$

Note that G drops out of (3.1) upon setting $h=0$. This would have to be the case in the boson analogy, since setting $h=0$ neglects quantum mechanics by decoupling the momentum from the position. The constraint (1.3) is unimportant in this classical limit.

In the limit $G \to \infty$, we recover the correlations typical of infinite polymers with no heads or tails from (3.1),

$$S(q_\perp, q_z) = \frac{k_B T q_\perp^2}{(h + \alpha q_\perp^2)\, q_z^2 + bq_\perp^2 + q_\perp^4} \tag{3.2}$$

For small momenta, we can examine the curves of constant $S(q_\perp, q_z)$. It is easy to see that these curves will go into the origin on straight lines, i.e., $q_z \sim q_\perp$. This is a generic feature expected to hold for all systems with the morphology of directed polymers, where the direction is explicitly chosen by an external field. Recalling that the limit as $|q| \to 0$ of the structure function is related to the compressibility of the sample (e.g., ref. 23), we can determine the compressibility of a sample of directed lines, which will depend on the direction of the compression.[6] Upon considering a compressional wave at an angle ϕ from the z axis, we take the momentum to be $q_z = q\cos\phi$ and $q_\perp = q\sin\phi$, and find, for small q,

$$S(q_\perp, q_z) \underset{q \to 0}{\sim} \frac{k_B T}{b + h(\cot\phi)^2} = k_B T \chi_T(\phi) \tag{3.3}$$

where χ_T is the compressibility, and is a function of the direction ϕ in which the compression is made. Note again that the $h=0$ limit is especially simple: The compressibility no longer depends on the compression angle if tangent fluctuations are ignored. We then recover the result for an isotropic fluid of point particles, namely $\chi_T = b^{-1}$. The compressibility enters the linear response relation:

$$\langle \delta\rho(q_\perp, q_z)\rangle = \chi(q_\perp, q_z)\, \delta\sigma(q_\perp, q_z) \tag{3.4}$$

[6] We thank Tom Witten for conversations on this point.

where $\delta\sigma$ is a sinusoidally varying force directed along $\vec{q}=(q_\perp, q_z)$. The unusual ϕ dependence of this response function may be understood as follows: Equations (3.4) and (3.3) predict that $\langle \delta\rho \rangle = 0$ for compressions when $\phi \to 0$. This result arises because squeezing the system along the z axis will not change the number of polymers piercing any constant z slice. In general, the linear response (3.4) depends on the directions of the compression relative to $\hat{z}$, as parametrized by ϕ.

Returning to finite-length polymers, and hence to finite G, we repeat the above analysis and find a ϕ-independent result

$$S(q_\perp, q_z) \underset{q \to 0}{\sim} \frac{k_B T}{b} \tag{3.5}$$

Because at sufficiently large distances (larger than the average polymer length l) finite-length polymers will ultimately behave like point particles, the long-wavelength properties of the sample will not exhibit any character of the directed constituents. At intermediate scales, the factors of $\mathcal{O}(Gq_\perp^2)$ may not be neglected in (3.1), and we return to the direction-dependent result (3.3).

4. RENORMALIZATION GROUP AND FINITE LENGTH POLYMERS

In the last section we saw that at long wavelengths the linelike nature of the directed melt disappears for finite chain lengths. Here we construct a renormalization group which allows us to study this crossover in detail. When $G \to \infty$, we recover the results of Larkin and Khmel'nitskiĭ.[9] For G finite, however, the system crosses over to the behavior of a $(d+1)$-dimensional Ising model with short-range interactions.[21] We shall treat the z direction separately from the directions in the plane perpendicular to z. We let d be the dimension of the *bosons* so that the corresponding directed polymers exist in $(d+1)$ dimensions (see Fig. 1).

Consider first the graph which renormalizes the four-point interaction $\delta\rho^4$. To interpret this graph we need to invert a $(d+1)\times(d+1)$ matrix to get the propagator, as there are d degrees of freedom in $\mathbf{t}$ and an additional degree of freedom from the density fluctuations, $\delta\rho$. However, as mentioned earlier, the transverse modes of $\mathbf{t}$ decouple. To make this explicit, we decompose $\mathbf{t}$ in momentum space,

$$\mathbf{t}(q_\perp, q_z) = \mathbf{t}_L + \mathbf{t}_T \tag{4.1}$$

with

$$t_{L,j} = \frac{q_j q_k}{q_\perp^2} t_k \tag{4.2}$$

and

$$t_{T,j} = \left(\delta_{jk} - \frac{q_j q_k}{q_\perp^2}\right) t_k \tag{4.3}$$

In (4.2) and (4.3) the indices j and k only run over the d-dimensional space perpendicular to z and we use the summation convention. Additionally, we take $t_{L,j} = -iq_j \pi(q_\perp, q_z)$. With this parametrization, the Fourier transform of the divergence of $\mathbf{t}$ is simply $i\mathbf{q}_\perp \cdot \mathbf{t} = q_\perp^2 \pi$, and the Fourier transform of the $\mathbf{t}^2$ term in (1.8) is

$$\int dq_z \, d^d q_\perp [q_\perp^2 \pi^2 + \mathbf{t}_T^2 - \frac{1}{q_\perp^2} (q_\perp \cdot \mathbf{t}_T)^2]$$

Thus we can integrate out $\mathbf{t}_T$ from (1.8), and we are left with a theory only involving $\delta\rho$ and π.

Inverting the 2×2 quadratic form which remains gives the following useful propagators:

$$\langle |\delta\rho(q_\perp, q_z)|^2 \rangle = \frac{h + Gq_\perp^2}{(G\alpha q_\perp^2 + Gh + \alpha h) q_z^2 + (Gb + h) q_\perp^2 + Gq_\perp^4 + hb} \tag{4.4a}$$

$$\langle |\pi(q_\perp, q_z)|^2 \rangle = \frac{1}{q_\perp^2} \frac{q_\perp^2 + b + \alpha q_z^2 + Gq_z^2}{(G\alpha q_\perp^2 + Gh + \alpha h) q_z^2 + (Gb + h) q_\perp^2 + Gq_\perp^4 + hb} \tag{4.4b}$$

$$\langle \delta\rho^*(q_\perp, q_z) \, \pi(q_\perp, q_z) \rangle = \frac{iGq_z}{(G\alpha q_\perp^2 + Gh + \alpha h) q_z^2 + (Gb + h) q_\perp^2 + Gq_\perp^4 + hb} \tag{4.4c}$$

After inserting these propagators into the graph shown in Fig. 5, we integrate out the frequency-like variable q_z and find that the renormalized four-point interaction associated with Eq. (1.8) is $c_R = c + \delta c + \mathcal{O}(c^3)$, where

$$\delta c = -\frac{3c^2}{8} \frac{2}{\Gamma(d/2)(4\pi)^{d/2}} \int \frac{q_\perp^{d-1} \, dq_\perp}{q_\perp^2} \times \frac{(1 + h/Gq_\perp^2)^{1/2}}{(h + \alpha q_\perp^2 + \alpha(h/G)^{1/2} [(1 + b/q_\perp^2)^3]^{1/2}} \tag{4.5}$$

Near the critical point, $b \approx 0$, and so when $G = \infty$, δc diverges in the infrared for $d \leqslant 2$. This infrared divergence suggests an ε-expansion around

Fig. 5. Hartree graph which diverges for $d<2$. We integrate here over all internal momenta.

$d=2$, where $\varepsilon=2-d$. Our approach follows ref. 24, which is a variation of the dynamic renormalization group of ref. 25. First we integrate out a momentum shell in $q_\perp$ from Λe^{-l} to Λ, but integrate freely over q_z. We then rescale our variables so that the ultraviolet cutoff in the perpendicular direction is held fixed. After rescaling ρ and $\mathbf{t}$ accordingly, we are left with the same theory but with different coupling constants. When this procedure is iterated, c is driven toward a fixed point which describes the universal long-wavelength critical behavior for large G.

4.1. Momentum Shell Integration

We must first integrate out the transverse momentum in the range $\Lambda e^{-l}<q_\perp<\Lambda$. This can be done straightforwardly by expanding the functional integral in c. Care must be taken to account for all possible contractions of the operators in the expansion. The symmetry factors can be found in the usual way for Wick expansions. It is important to note that diagrams renormalize the remaining low-momentum modes, and are not simply expectation values. Graphs which renormalize the quadratic and quartic contributions to Landau theory are shown in Fig. 6. Upon carrying out this procedure, we arrive at the following relations for the intermediate values of the coupling constants in (1.8):

$$h'=h \tag{4.6a}$$

$$\alpha'=\alpha \tag{4.6b}$$

$$b'=b+\frac{c}{4\sqrt{G}}\int_{\Lambda e^{-l}}^{\Lambda}\frac{d^dq_\perp}{(2\pi)^d}\left[\frac{(h+Gq_\perp^2)^{1/2}}{(b+q_\perp^2)^{1/2}}\frac{1}{(h+\alpha q_\perp^2+\alpha(h/G))^{1/2}}\right] \tag{4.6c}$$

$$c'=c\left(1-\frac{3c}{8\sqrt{G}}\int_{\Lambda e^{-l}}^{\Lambda}\frac{d^dq_\perp}{(2\pi)^d}\times\left[\frac{(h+Gq_\perp^2)^{1/2}}{[(b+q_\perp^2)^3]^{1/2}}\frac{1}{(h+\alpha q_\perp^2+\alpha(h/G))^{1/2}}\right]\right) \tag{4.6d}$$

$$G'=G \tag{4.6e}$$

where we have gone to one-loop order. In (4.6) we have already integrated over q_z.

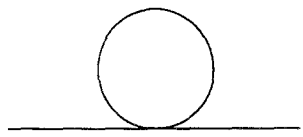

(a)

(b)

Fig. 6. Graphs which contribute to the renormalization group calculation. In these graphs, the internal lines are integrated over all values of q_z, but $q_\perp$ is only integrated in a momentum shell between Λe^{-l} and Λ. (a) A graph which renormalizes the propagator; (b) a graph which renormalizes the four-point coupling c.

We rescale perpendicular lengths by $R'_\perp = R_\perp e^{-l}$ and the z direction by

$$Z' = Z \exp\left[-\int_0^l \gamma(l')\, dl' \right]$$

In momentum space, these rescalings read $q'_\perp = q_\perp e^l$ and

$$q'_z = q_z \exp\left[\int_0^l \gamma(l')\, dl' \right]$$

where the function $\gamma(l)$ is to be determined.

When doing the first momentum shell integration, the coupling constants were independent of length scale. However, they then acquire a momentum dependence because we have absorbed the large momentum effects into them. The correct renormalized theory is a coupled set of integral equations where the coupling constants are taken to be scale dependent. An alternative, but equivalent approach is to integrate over a small momentum range where the coupling constants are approximately fixed and then repeat the entire calculation iteratively. This leads to the usual differential renormalization group equations.

4.2. Recursion Relations and Critical Behavior

We now choose an infinitesimal momentum shell $e^{-\delta}$ and take the limit $\delta \to 0$. This leads to differential renormalization group equations which can be integrated to produce the couplings appropriate for a cutoff Λe^{-l} in the perpendicular direction. We use units such that $\Lambda = 1$ in the following. We also define the renormalized "reduced temperature"

$$r = b + \frac{c}{2(h+\alpha)^{1/2}} A_d \tag{4.7}$$

which vanishes at the critical point in the fluctuation-corrected theory. The constant $A_d = 2/\Gamma(d/2)(4\pi)^{d/2}]$ is a geometrical factor. The differential recursion relations valid near $d = 2$ are

$$\frac{dh(l)}{dl} = h(4-2\gamma) \tag{4.8a}$$

$$\frac{d\alpha(l)}{dl} = a(2-2\gamma) \tag{4.8b}$$

$$\frac{dr(l)}{dl} = r\left(2 - \frac{c}{16\pi(h+\alpha+\alpha(h/G)^{1/2}}\right) + \frac{ch}{16\pi G(h+\alpha+\alpha(h/G)^{1/2}} \tag{4.8c}$$

$$\frac{dc(l)}{dl} = c\left(4-d-\gamma - \frac{3c}{16\pi(h+\alpha+\alpha(h/G)^{1/2}}\right) \tag{4.8d}$$

$$\frac{dG(l)}{dl} = G(2-2\gamma) \tag{4.8e}$$

We set $\gamma = 2$ in order to hold h fixed, and note that α is an irrelevant variable. We have expanded about $G^{-1} = 0$. Examining these recursion relations, we see that perturbation theory amounts to an expansion in two parameters, namely $\bar{c} = c(h+\alpha(h/G)^{1/2}$ and $(\bar{G})^{-1} = hG^{-1}$. These couplings have the recursion relations

$$\frac{d\bar{c}}{dl} = \bar{c}\left(\varepsilon - \frac{3\bar{c}}{16\pi}\right) \tag{4.9a}$$

$$\frac{d}{dl}\left(\frac{h}{G}\right) = 2\left(\frac{h}{G}\right) \tag{4.9b}$$

where $\varepsilon = 2-d$.

We first consider the subspace of theories with $G = \infty$. In this case there is a stable, nontrivial fixed point for positive ε. Though we have

already noted that this theory is identical to the uniaxial ferroelectric, and hence should have all the same critical behavior, a direct calculation of these exponents provides a useful check of our renormalization group method. In particular we can calculate the logarithmic corrections to the compressibility discussed in Section 3 in the critical dimension of $2+1=3$. Upon setting $\varepsilon=0$ in (4.9a) we solve for $\bar{c}(l)$ and find that

$$\bar{c}(l)=\frac{\bar{c}(0)}{1+[3\bar{c}(0)/16\pi]\,l} \tag{4.10}$$

which leads via (4.8c) to

$$r(l)=r(0)\,e^{2l}\left(1+\frac{3\bar{c}(0)}{16\pi}\,l\right)^{-1/3} \tag{4.11}$$

Since at this order in ε there is no nontrivial rescaling of the fields, we have

$$\begin{aligned}
&\chi(q_\perp, q_z; r_0)\\
&\quad=\int dz\, d^dx[\exp(iq_\perp\cdot\mathbf{x}-iq_z z)]\langle\rho(\mathbf{x}, z)\,\rho(\mathbf{0}, 0)\rangle_{l=0}\\
&\quad=\int \exp\left[\int_0^l \gamma(l')\,dl'\right]dz'\exp(dl)\,d^dx'\\
&\qquad\times\left(\exp\left[-\tfrac{1}{2}\int_0^l\gamma(l')\,dl'\right]\exp[(2-d)\,l/2]\right)^2\\
&\qquad\times[\exp(iq'_\perp\cdot\mathbf{x}'-iq'_z z')]\langle\rho'(\mathbf{x}', z)\,\rho'(\mathbf{0}, 0)\rangle_l\\
&\quad=(\exp 2l)\,\chi_l\left((\exp l)\,q_\perp, \left\{\exp\left[\int_0^l\gamma(l')\,dl'\right]\right\}q_z; r(l)\right)
\end{aligned} \tag{4.12}$$

We now choose $l=l^*$ large enough so that $r(l^*)$ has grown to $\mathcal{O}(1)$. Then we have from (4.11)

$$1=r(l^*)=r_0(3\bar{c}_0/16\pi)^{-1/3}\,e^{2l^*}(l^*)^{-1/3} \tag{4.13}$$

so that

$$e^{2l^*}\sim r_0^{-1}\,|\ln r_0|^{1/3} \tag{4.14}$$

and thus

$$\chi(q_\perp, q_z; r_0)=\frac{|\ln r_0|^{1/3}}{r_0}\,\chi(\xi_\perp q_\perp, \xi_z q_z; 1) \tag{4.15}$$

where $\xi_\perp^2 \sim \xi_z \sim (\ln r_0)^{1/3}/r_0$, in agreement with the results of ref. 9. Note the anisotropically diverging correlation lengths produced by the directed line-like nature of the degrees of freedom. The two-loop calculation of ref. 26 leads to the result $\xi_z \sim \xi_\perp^{2-2\varepsilon^2/243}$ to $\mathcal{O}(\varepsilon^2)$. Recalling the discussion in the last section of the compressibility, we have finally

$$\chi(q \sin\phi, q\cos\phi; r_0) \underset{q\to 0}{\sim} \frac{|\ln r_0|^{1/3}}{r_0} \frac{1}{1+h(|\ln r_0|^{1/3}/r_0)(\cot\phi)^2} \tag{4.16}$$

which should be compared to the mean field result (3.3). Note that the effective direction of the compressional wave changes as we go to longer length scales. Near the critical point we always find $\chi(\phi) \sim 1/[h(\cot\phi)^2]$, which appears to be a universal result.

Similarly, in the ordered phase, we can calculate the specific heat exponent by flowing along a renormalization group trajectory and matching on to an effective free energy at long wavelengths (a more complicated calculation shows that this behavior occurs above T_C as well). In the ordered phase, the bulk free energy is approximately $-3\Omega(r^2/2c)$, where Ω is the total volume of the system. We then have

$$\begin{aligned} F_l &= -3\Omega_l \frac{r(l)^2}{2c(l)} \\ &= -\frac{3}{2}\left\{\exp(-dl)\exp\left[-\int_0^l \gamma(l')\,dl'\right]\right\}\Omega_0 \frac{r(l)^2}{c(l)} \end{aligned} \tag{4.17}$$

Again choosing $l = l^*$ as in (4.13), we find that

$$\begin{aligned} F_l &= -\frac{3}{2}\left\{\exp(-dl^*)\exp\left[-\int_0^{l^*} \gamma(l')\,dl'\right]\right\}\Omega_0 \frac{1^2}{c(l^*)} \\ &\sim \{\exp[-(d+2)\,l^* \sim r_0^2\,|\ln r_0|^{1/3} \end{aligned} \tag{4.18}$$

Differentiating twice with respect to r_0, we recover the correct specific heat-like behavior at the critical point.

Going back to the full theory, we now allow G^{-1} to take on finite values. In this case we are driven away from our fixed point and G^{-1} flows toward ∞. This reflects a crossover to an anisotropic but *pointlike* phase where the constraint (1.3), and hence the linelike nature of the polymers, is unimportant. Because **t** decouples from the density fluctuations, the quantum mechanical bosons behave classically at long wavelengths. A similar crossover occurs in polymer nematics when hairpins are introduced into the theory and the previously directed polymers become isotropic.[4]

5. MIXING EXPONENTS

We now consider directed polymer blends, or, equivalently, binary mixtures of two superfluids. As with binary mixing in classical systems of point particles, the mixing exponents are identical to the liquid–gas exponents. We demonstrate this equivalence by showing that the Landau–Ginzburg theory controlling the mixing fraction is the same as that for a single-component critical point, (1.1). For simplicity, we restrict our attention to the limit $G \to \infty$. In Appendix A we derive the quadratic part of the free energy of two polymer species using the boson representation. To these terms we add nonlinear couplings to account for the configurational entropy of each polymer species, multiparticle interactions, etc., and consider the model free energy

$$F = \int dz\, d^d x \left[\begin{array}{l} \dfrac{h_1}{2}\mathbf{t}_1^2 + \dfrac{h_2}{2}\mathbf{t}_2^2 + h_{12}\mathbf{t}_1 \cdot \mathbf{t}_2 + \dfrac{1}{2}(\nabla_\perp \delta\rho_1)^2 \\ \quad + \dfrac{1}{2}(\nabla_\perp \delta\rho_2)^2 + \dfrac{b_1}{2}\delta\rho_1^2 + \dfrac{b_2}{2}\delta\rho_2^2 + b_{12}\delta\rho_1\delta\rho_2 + \dfrac{w_1}{3!}\delta\rho_1^3 \\ \quad + \dfrac{w_2}{3!}\delta\rho_2^3 + \dfrac{c_1}{4!}\delta\rho_1^4 + \dfrac{c_2}{4!}\delta\rho_2^4 + \dfrac{c_{12}}{4}\delta\rho_1^2\delta\rho_2^2 \end{array} \right] \tag{5.1}$$

subject to the constraints

$$\partial_z \delta\rho_j + \nabla_\perp \cdot \mathbf{t}_j = 0, \qquad j = 1, 2 \tag{5.2}$$

As with isotropic polymer melts, the energy of two polymers of length L scales like L, while the entropy of mixing is independent of L, which leads to phase separation at all temperatures when $L \to \infty$. To insure a finite temperature phase transition, we rescale the bare mixing energy, χ, by L^{-1}, thus setting $b_{12} = \chi/L$. The same caveat applies to quantum bosons when we set $b_{12} = \chi/\beta\hbar$. We have neglected gradient terms of the form $(\partial_z \delta\rho_i)^2$, because these turn out to be irrelevant at the demixing point. Terms proportional to $\delta\rho_1\delta\rho_2^2$ and $\delta\rho_2\delta\rho_1^2$ could have been added, but do not affect our results in any essential way. Additionally, we assume that the $(\nabla_\perp \delta\rho_i)^2$ terms have been diagonalized so that the term $\nabla_\perp \delta\rho_1 \cdot \nabla_\perp \delta\rho_2$ is not present. It is useful to pass to sum and difference variables, i.e., $\delta\rho_\pm = (\delta\rho_1 \pm \delta\rho_2)/\sqrt{2}$. We only keep terms in the free energy up to second order in the noncritical mode $\delta\rho_+$, but keep all terms up to quartic order in $\delta\rho_-$. We also define fields $\mathbf{t}_\pm = (\mathbf{t}_1 \pm \mathbf{t}_2)/\sqrt{2}$ which are the tangents associated with the sum and difference variables. The free energy now takes the form

$$F=\int dz\, d^dx \left[\begin{array}{l} \frac{h_+}{2}\mathbf{t}_+^2+\frac{h_-}{2}\mathbf{t}_-^2+h_{+-}\mathbf{t}_+\mathbf{t}_-+\frac{1}{2}(\nabla_\perp\delta\rho_+)^2 \\ \quad +\frac{1}{2}(\nabla_\perp\delta\rho_-)^2+\frac{b_+}{2}\delta\rho_+^2+\frac{b_-}{2}\delta\rho_-^2 \\ \quad +b_{+-}\delta\rho_+\delta\rho_-+\frac{w_-}{3!}\delta\rho_-^3+\frac{c_-}{4!}\delta\rho_-^4 \end{array}\right] \tag{5.3}$$

with the constraints now reading

$$\partial_z\delta\rho_\pm+\nabla_\perp\cdot\mathbf{t}_\pm=0 \tag{5.4}$$

We can again integrate out the transverse parts of $\mathbf{t}_\pm$ and use the constraint (5.4) to solve for the longitudinal parts. The resulting quadratic part of the free energy reads (in momentum space)

$$F_{\text{quad}}=\int\frac{dq_z}{2\pi}\frac{d^dq_\perp}{(2\pi)^d}\left[\begin{array}{l} \frac{1}{2}\left(h_+\frac{q_z^2}{q_\perp^2}+q_\perp^2+b_+\right)|\delta\rho_+|^2 \\ \quad +\frac{1}{2}\left(h_-\frac{q_z^2}{q_\perp^2}+q_\perp^2+b_-\right)|\delta\rho_-|^2 \\ \quad +h_{+-}\frac{q_z^2}{q_\perp^2}\delta\rho_+\delta\rho_-+b_{+-}\delta\rho_+\delta\rho_- \end{array}\right] \tag{5.5}$$

At this point we are in the position to integrate out $\delta\rho_+$, resulting in

$$F'_{\text{quad}}[\delta\rho_-]=\frac{1}{2}\int\frac{dq_z}{2\pi}\frac{d^dq_\perp}{(2\pi)^d} \times\left[h_-\frac{q_z^2}{q_\perp^2}+q_\perp^2+b_--\frac{(h_{+-}(q_z^2/q_\perp^2)+b_{+-})^2}{h_+(q_z^2/q_\perp^2+q_\perp^2+b_+}\right]|\delta\rho_-|^2 \tag{5.6}$$

Upon expanding the denominator of (5.6) in $q_\perp$ and q_z, keeping only relevant and marginally relevant terms, and reintroducing $\mathbf{t}_-$, we finally have

$$F'=\int dz\, d^dx \left[\begin{array}{l} \frac{1}{2}\left(h_--\frac{2b_{+-}h_{+-}}{b_+}+\frac{b_{+-}^2h_+}{b_+^2}\right)\mathbf{t}_-^2 \\ \quad +\frac{1}{2}\left(1+\frac{b_{+-}^2}{b_+^2}\right)(\nabla_\perp\delta\rho_-)^2+\frac{1}{2}\left(b_--\frac{b_{+-}^2}{b_+}\right) \\ \quad \times\delta\rho_-^2+\frac{w_-}{3!}\delta\rho_-^3+\frac{c_-}{4!}\delta\rho_-^4 \end{array}\right] \tag{5.7}$$

subject to

$$\partial_z\delta\rho_-+\nabla_\perp\cdot\mathbf{t}_-=0 \tag{5.8}$$

As in the single-component model, the critical mixing line is obtained by setting $w_- = 0$. This could be done by altering the chemical potentials of the two species, for instance. Our model is thus equivalent to the original model (1.1), except for the unimportant coupling $\alpha(\partial_z \delta\rho_-)^2$. We conclude that the critical mixing of *linelike* objects is also in the universality class of the three-dimensional uniaxial ferroelectric.

APPENDIX A. DERIVATION OF HYDRODYNAMICS FOR BINARY MIXTURES

Our starting point is a pair of boson field theories, each describing a distinct superfluid or polymer species.[2] We then couple them through their densities, as well as their "currents" or tangent fields. More precisely, the partition function is

$$Z = \int [d\psi_1^*][d\psi_1][d\psi_2^*][d\psi_2] \exp(-S[\psi_1^*, \psi_1, \psi_2^*, \psi_2]) \tag{A.1}$$

where the action is

$$\frac{F}{k_B T} \equiv S = S_1[\psi_1^*, \psi_1] + S_2[\psi_2^*, \psi_2] + S_{12}[\psi_1^*, \psi_1, \psi_2^*, \psi_2] \tag{A.2}$$

The individual terms read

$$S_j = \int dz\, d^d x \left[\psi_j^* (\partial_z - D_j \nabla_\perp^2 - \bar{\mu}_j)\, \psi_j + \frac{B_j}{4} |\psi_j|^4 \right] \tag{A.3}$$

while the interaction is

$$\begin{aligned} S_{12} = \int dz\, d^d x [& B_{12} |\psi_1|^2 |\psi_2|^2 \\ & + \eta_{12} (\psi_1^* \nabla_\perp \psi_1 - \psi_1 \nabla_\perp \psi_1^*) \cdot (\psi_2^* \nabla_\perp \psi_2 - \psi_2 \nabla_\perp \psi_2^*)] \end{aligned} \tag{A.4}$$

The change of variables

$$\psi_j = \sqrt{\rho_j}\, e^{i\theta_j} \tag{A.5}$$

leads to

$$S = \int dz\, d^d x \left\{ \begin{aligned} & i\rho_1 \partial_z \theta_1 + \frac{D_1 (\nabla_\perp \rho_1)^2}{4\rho_1} + D_1 \rho_1 (\nabla_\perp \theta_1)^2 \\ & - \bar{\mu}_1 \rho_1 + \frac{B_1}{4} \rho_1^2 + i\rho_2 \partial_z \theta_2 + \frac{D_2 (\nabla_\perp \rho_2)^2}{4\rho_2} \\ & + D_2 \rho_2 (\nabla_\perp \theta_2)^2 - \bar{\mu}_2 \rho_2 + \frac{B_2}{4} \rho_2^2 \\ & + B_{12} \rho_1 \rho_2 + \eta_{12} \rho_1 \rho_2 \nabla_\perp \theta_1 \cdot \nabla_\perp \theta_2 \end{aligned} \right\} \tag{A.6}$$

We now introduce two fields which we shall see are proportional to the tangent fields of the individual species. We start with the identity

$$\exp\left\{\int dz\, d^dx[D_1\rho_1(\nabla_\perp\theta_1)^2+D_2\rho_2(\nabla_\perp\theta_2)^2+\eta_{12}\rho_1\rho_2\nabla_\perp\theta_1\cdot\nabla_\perp\theta_2]\right\}$$

$$=\int[d\mathbf{p}_1][d\mathbf{p}_2]\exp\left\{\int dz\, d^dx\left[\begin{array}{c}\dfrac{D_2\rho_2\mathbf{p}_1^2+D_1\rho_1\mathbf{p}_2^2-2\eta_{12}\rho_1\rho_2\mathbf{p}_1\cdot\mathbf{p}_2}{D_1D_2\rho_1\rho_2-\eta_{12}^2\rho_1^2\rho_2^2}\\ +i\mathbf{p}_1\cdot\nabla_\perp\theta_1+i\mathbf{p}_2\cdot\nabla_\perp\theta_2\end{array}\right]\right\} \tag{A.7}$$

Upon using this identity to replace the terms quadratic in θ appearing in (A.6) and integrating over θ_j, we find that

$$Z=\int[d\rho_1][d\rho_2][d\mathbf{p}_1][d\mathbf{p}_2]$$

$$\times\delta[\partial_z\rho_1+\nabla_\perp\cdot\mathbf{p}_1]\,\delta[\partial_z\rho_2+\nabla_\perp\cdot\mathbf{p}_2]\exp(-S'[\rho_1,\rho_2,\mathbf{p}_1,\mathbf{p}_2]) \tag{A.8}$$

where

$$S'=\int dz\, d^dx\left\{\begin{array}{l}\dfrac{D_2\rho_2\mathbf{p}_1^2+D_1\rho_1\mathbf{p}_2^2-2\eta_{12}\rho_1\rho_2\mathbf{p}_1\cdot\mathbf{p}_2}{D_1D_2\rho_1\rho_2-\eta_{12}^2\rho_1^2\rho_2^2}\\ \quad+\dfrac{D_1(\nabla_\perp\rho_1)^2}{4\rho_1}+\dfrac{D_2(\nabla_\perp\rho_2)^2}{4\rho_2}\\ \quad-\bar{\mu}_1\rho_1-\bar{\mu}_2\rho_2+\dfrac{B_1}{4}\rho_1^2+\dfrac{B_2}{4}\rho_2^2+B_{12}\rho_1\rho_2\end{array}\right\} \tag{A.9}$$

We now expand $\rho_i=\rho_{0,i}+\delta\rho_i$ around the minimum of the bulk free energy and rescale $\delta\rho_j$ so that the kinetic term in the action is $(1/2k_BT)(\nabla_\perp\delta\rho_j)^2$ to obtain

$$S'=\frac{1}{k_BT}\int dz\, d^dx\left\{\begin{array}{l}\dfrac{h_1}{2}\mathbf{t}_1^2+\dfrac{h_2}{2}\mathbf{t}_2^2+h_{12}\mathbf{t}_1\cdot\mathbf{t}_2\\ \quad+\dfrac{1}{2}(\nabla_\perp\delta\rho_1)^2+\dfrac{1}{2}(\nabla_\perp\delta\rho_2)^2\\ \quad+\dfrac{b_1}{2}\delta\rho_1^2+\dfrac{b_2}{2}\delta\rho_2^2+b_{12}\delta\rho_1\delta\rho_2\end{array}\right\} \tag{A.10}$$

where $\mathbf{t}_j = (D_j/2\rho_{j,0})^{1/2}\,\mathbf{p}_j$ and the h_j and b_j can be read off from (A.9) in the expansion of ρ_j around $\rho_{j,0}$. The delta functionals in (A.8) impose the constraints

$$\partial_z \delta\rho_j + \nabla_\perp \cdot \mathbf{t}_j = 0 \tag{A.11}$$

APPENDIX B. QUANTUM TRICRITICAL POINTS

Although somewhat outside the main scope of this paper, we summarize here another problem in zero-temperature quantum critical phenomena which is soluble by the coherent-state path integral methods.[29-30] For purely repulsive pair potentials, the phase diagram for interacting bosons is expected to be as shown in Fig. 7a.[7] Helium-like potentials with a

[7] See for example, ref. 27. The same phase diagram was applied to high-temperature superconductors in ref. 2.

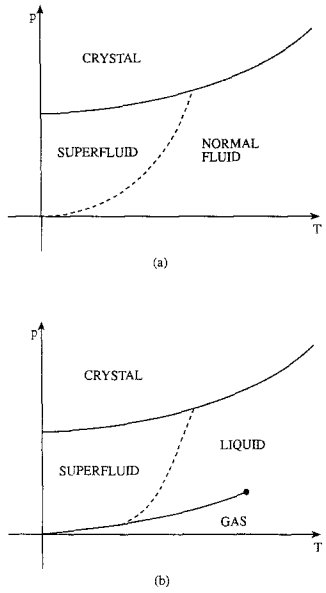

Fig. 7. Schematic pressure–temperature phase diagram for (a) bosons with a purely repulsive potential, and (b) bosons with a single minimum deep enough to produce first-order liquid–gas coexistence at finite temperatures. As the depth of the minimum is decreased, we expect that the liquid–gas critical point in (b) recedes toward low temperatures, eventually becoming a tricritical point separating the lambda line from a first-order transition from gas to superfluid. The quantum tricritical point discussed in Appendix B arises when this finite-temperature tricritical point just reaches $T = 0$. Further decrease in the minimum (or an increase in $\hbar$) leads to the phase diagram in (a).

sufficiently deep single minimum, on the other hand, lead to the familiar phase diagram of Fig. 7b. At $T=0$ and zero pressure, there is a continuous transition from a vacuum to a superfluid gas for repulsive potentials.[30] The corresponding transition from a vacuum to a superfluid *liquid* for helium-like potentials is strongly first order. As the depth of the single minimum in a helium-like potential is decreased (or as $\hbar$ is increased), this first-order transition should weaken, ultimately becoming continuous at some point. This changeover is described by a tricritical point within the coherent-state path integral formalism.

To see how this quantum tricritical point arises, we generalize the path integral used to describe d-dimensional superfluid gases in ref. 30,

$$\int [d\psi^*][d\psi] \exp(-S[\psi^*, \psi]/\hbar) \tag{B.1}$$

where the "action" is

$$S/\hbar = \int dz\, d^d x[\psi^*(\partial_z - D\nabla_\perp^2)\,\psi - \mu\,|\psi|^2 + u\,|\psi|^4 + v\,|\psi|^6] \tag{B.2}$$

Here, D is the quantum "diffusion constant" related to the boson mass by $D=\hbar/m$, and μ is the chemical potential. The coupling u describes pairwise interactions, while v represents three-body terms. If u is positive, the potential is predominantly repulsive in the dilute limit and the vacuum ($\psi=0$) to superfluid gas ($\psi\neq 0$) transition occurs at $\mu=0$ within mean field theory. Mean field theory correctly describes the continuous transition in all dimensions greater than $d=2$, where there are logarithmic corrections.[28]

For u negative, on the other hand, the predominant pairwise interaction is attractive. One must now appeal to a positive sixth-order term to stabilize the functional integral. Upon minimizing the sixth-order polynomial part of (B.2), one then finds that mean field theory predicts a first-order transition from $\psi=0$ to $\psi\neq 0$ at a chemical potential given by

$$-\mu = \frac{u^2}{4v} \tag{B.3}$$

A closely related analysis describes finite-temperature phase separation in He^3–He^4 mixtures.

The boundary between regimes of continuous and first-order transitions from the vacuum occurs at a tricritical point located within mean field theory at $\mu=0$ and $u=0$.[8] Fluctuations alter the mean field predic-

[8] For a discussion of finite-temperature tricritical points in ^{3}He–^{4}He mixtures, see ref. 31.

tions for ordinary thermal tricritical points only for $d<3$; there are logarithmic corrections for $d=3$. It is easy to check that the anisotropic gradient terms in the quantum tricritical action (B.2) do not alter the mean field tricritical exponents for *either* two- or three-dimensional quantum systems.

There are two contexts in which these observations may become experimentally relevant. The first was discussed by Cheng *et al.*,[18] who proposed to use the substrate to alter the effective interparticle potential in helium films. The second arises from work by Muzikar and Pethicke,[17] who found circumstances under which the interaction between vortices could become attractive for type II superconductors. This converts the usual continuous transition at H_{C1} to a first-order transition. The boundary between these two possibilities is exactly the quantum tricritical point discussed in this Appendix, for the case of two-dimensional bosons. The Meissner phase for superconductors corresponds to the vacuum discussed above.[2] In practice, the first-order transition of Muzikar and Pethicke may only occur at relatively low temperatures. Once the entropic penalty for confinement in the potential well becomes comparable to the well depth, we expect the transition to become continuous again. The equivalent criterion for quantum systems is that the zero-point energy be larger than the depth of the minimum in the pair potential. The "quantum" tricritical point discussed here would then appear in type II superconductors as a point on the H_{C1} line separating a low-temperature first-order transition from a high-temperature continuous one.

ACKNOWLEDGMENTS

It is a pleasure to acknowledge helpful conversation with L. Balents, P. Clark, M. Cole, B. I. Halperin, T. Hwa, P. Le Doussal, G. McKinley, R. B. Meyer, S. Milner, O. Narayan, and T. Witten during the course of this investigation. One of us (R.D.K.) would like to acknowledge the support of a National Science Foundation Graduate Fellowship. This work was supported by the National Science Foundation, through Grant DMR91-15491 and through the Harvard Materials Research Laboratory.

REFERENCES

1. R. P. Feynman, *Phys. Rev.* **91**:1291 (1953); see also R. P. Feynman and A. R. Hibbs, *Quantum Mechanics and Path Integrals* (McGraw-Hill, New York, 1965); R. P. Feynman, *Statistical Mechanics*, (Benjamin/Cummins, Reading, Massachusetts, 1972).
2. D. R. Nelson, *Phys. Rev. Lett.* **60**:1973 (1988); D. R. Nelson and H. S. Seung, *Phys. Rev. B* **39**:9153 (1989); D. R. Nelson and P. Le Doussal, *Phys. Rev. B* **42**:10113 (1990).

3. P. Le Doussal and D. R. Nelson, *Europhys. Lett.* **15**:161 (1991).
4. R. D. Kamien, P. Le Doussal, and D. R. Nelson, *Phys. Rev. A* **45**:8727 (1992).
5. D. R. Nelson, *Physica A* **177**:220 (1991).
6. P. G. de Gennes, *J. Phys Lett.* (Paris) **36L**:55 (1975).
7. M. C. Marchetti and D. R. Nelson, *Phys. Rev. B* **42**:9938 (1990); *Physica C* **174**:40 (1991).
8. J. V. Selinger and R. F. Bruinsma, *Phys. Rev. A* **43**:2910 (1991).
9. A. I. Larkin and D. E. Khmel'nitskiĭ, *Zh. Eksp. Teor. Fig.* **29**:1123 (1969); see also A. Aharony, *Phys. Rev. B* **8**:3363 (1973); **9**:3946 (E) (1974).
10. P. G. de Gennes, *Physics of Liquid Crystals* (Oxford University, Oxford, 1974).
11. T. C. Halsey and W. Toor, *J. Stat. Phys.* **61**:1257 (1990).
12. T. C. Halsey and W. Toor, *Phys. Rev. Lett.* **65**:2820 (1990).
13. G. C. Maitland, M. Rigby, E. B. Smith, and W. Wakeham, *Intermolecular Forces* (Clarendon Press, Oxford, 1981).
14. R. Tao, Southern Illinois University Preprint (1992).
15. T. Chen, R. N. Zitter, and R. Tao, Southern Illinois University Preprint (1992).
16. A. P. Gast and C. F. Zukoski, *Adv. Colloid Interface Sci.* **30**:153 (1989).
17. P. Muzikar and C. Pethicke, *Phys. Rev. B* **24**:2533 (1981).
18. E. Cheng, M. W. Cole, and P. B. Shaw, *J. Low Temp. Phys.* **79**:49 (1991).
19. D. Forster, *Hydrodynamic Fluctuations, Broken Symmetry and Correlation Functions* (Benjamin/Cummings, Reading, Massachusetts, 1975).
20. A. A. Abrikosov, L. P. Gorkov, and I. E. Dzyaloshinski, *Methods of Quantum Field Theory in Statistical Physics* (Dover, New York, 1963).
21. A. P. Young, *J. Phys. C* **8**:L309 (1975) and references therein.
22. See also Terry Hwa, unpublished.
23. R. K. Pathria, *Statistical Mechanics* (Pergamon, Exeter, England, 1972).
24. D. Forster, D. R. Nelson, and M. J. Stephen, *Phys. Rev. A* **16**:732 (1977).
25. B. I. Halperin, P. C. Hohenberg, and S. K. Ma, *Phys. Rev. Lett.* **29**:1548 (1972).
26. E. Brézin and J. Zinn-Justin, *Phys. Rev. B* **13**:251 (1976).
27. K. S. Liu and M. E. Fisher, *J. Low Temp. Phys.* **10**:655 (1973).
28. J. W. Negele and J. Orland, *Quantum Many-Particle Systems* (Addison-Wesley, New York, 1988).
29. V. N. Popov, *Functional Integrals and Collective Excitations* (Cambridge University Press, New York, 1987).
30. D. S. Fisher and P. C. Hohenberg, *Phys. Rev. B* **37**:4936 (1988), and references therein.
31. J. R. Rudnick and D. R. Nelson, *Phys. Rev. B* **13**:2208 (1976), and references therein.